Odd-parity pairing correlations in a *d*-wave superconductor

Jaechul Lee,[1] Satoshi Ikegaya,[2] and Yasuhiro Asano[1,3]
[1]*Department of Applied Physics, Hokkaido University, Sapporo 060-8628, Japan*
[2]*Max-Planck-Institut für Festkörperforschung, Heisenbergstrasse 1, D-70569 Stuttgart, Germany*
[3]*Center of Topological Science and Technology, Hokkaido University, Sapporo 060-8628, Japan*

(Received 19 November 2020; revised 3 March 2021; accepted 4 March 2021; published 15 March 2021)

We theoretically study the effects of spin-orbit interactions on the symmetry of a Cooper pair in a spin-singlet *d*-wave superconductor and on the chiral property of the surface Andreev bound states at zero energy. The pairing symmetry is analyzed by using the anomalous Green's function, which is obtained by solving the Gor'kov equation analytically. The chiral property of surface bound states is discussed by using an index that represents a number of zero-energy states in the presence of potential disorder at a surface. A spin-orbit interaction induces a spatially uniform spin-triplet *p*-wave pairing correlation in a superconductor and an odd-frequency spin-triplet *s*-wave pairing correlation at a surface. The spin-orbit interaction splits the Fermi surface into two depending on the spin configuration. As a result of splitting, the index can be a nontrivial nonzero value. On the basis of the close relationship among the odd-frequency *s*-wave pairing correlation at a surface, the nonzero index of surface bound states, and the anomalous proximity effect, we provide a design of a superconductor that causes the strong anomalous proximity effect.

DOI: 10.1103/PhysRevB.103.104509

I. INTRODUCTION

Proximity structures consisting of a dirty normal metal and spin-triplet superconductors indicate unusual electric transport properties such as the quantization of zero-bias conductance in a normal-metal/superconductor (NS) junction and the fractional current-phase relationship of the Josephson current in a superconductor/normal-metal/superconductor (SNS) junction [1,2]. Such unusual transport phenomena via a dirty normal metal are called the anomalous proximity effect. Topologically protected bound states at a surface of a spin-triplet superconductor play a key role in the anomalous proximity effect. Namely, they penetrate into a dirty normal metal and form the resonant transmission channels at the Fermi level, which causes the perfect electron transmission through the dirty normal metal [3–5]. The formation of the resonant states at the Fermi level can be detected directly as a large zero-energy peak in the local density of states (LDOS) [1,2] at a dirty normal metal. The anomalous proximity effect has been considered as a part of Majorana physics [6–10] because a spin-triplet superconductor hosts Majorana fermions at its surface. Unfortunately, well-established spin-triplet superconductors have not been discovered yet.

Tamura and Tanaka [11] have studied theoretically the LDOS at a dirty normal metal attached to a d_{xy}-wave superconducting film with the Rashba spin-orbit interaction, where the NS interface is parallel to the y direction as illustrated in Figs. 1(a)–1(c). Their numerical results indicate signs of the anomalous proximity effect. The modest enhancement of the LDOS at zero energy suggests the penetration of the zero-energy states (ZESs) into a dirty metal. In addition, they found an odd-frequency spin-triplet *s*-wave Cooper pair in the normal metal. (See recent review papers on odd-frequency pairing correlations [12,13].) Although the signal of the proximity effect is very weak, the results are highly nontrivial due to the following reasons: It has already been established in the absence of spin-orbit interactions that a d_{xy}-wave superconductor in Fig. 1(c) does not exhibit any proximity effect in a dirty metal [14–16]. Spin-orbit interaction may induce a spin-triplet Cooper pair in a spin-singlet superconductor [7,17–24]. However, mechanisms of symmetry conversion to an odd-frequency *s*-wave Cooper are still unclear.

In this paper, we theoretically study the effects of spin-orbit interactions in a spin-singlet d_{xy}-wave superconductor on the symmetry of a Cooper pair and on the chiral property of Andreev bound states at its surface. We analyze the symmetry of a Cooper pair by using the anomalous Green's function obtained by solving the Gor'kov equation analytically. The results show that a specific spin-orbit interaction generates a spin-triplet p_x-wave pairing correlation in bulk and an odd-frequency spin-triplet *s*-wave pairing correlation at a surface. The Bogoliubov–de Gennes (BdG) Hamiltonian of such a d_{xy}-wave superconductor preserves nontrivial chiral symmetry, which enables us to define an index by using the chiral eigenvalues of surface Andreev bound states at zero energy. We find that the index, a measure of the strength of the anomalous proximity effect, can be nonzero values only in the presence of the spin-orbit interaction. On the basis of the obtained results, we explain why the signs of the anomalous proximity effect in Ref. [11] are weak, and we provide a design for a superconductor that causes the strong anomalous proximity effect.

This paper is organized as follows. In Sec. II, we explain the anomalous proximity effect in more detail and three necessary conditions of the BdG Hamiltonian for the anomalous proximity effect. We also illustrate the goals of this paper. In

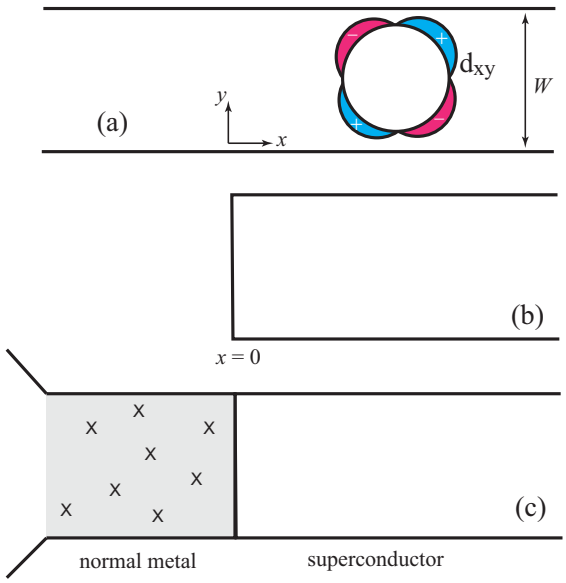

FIG. 1. Schematic pictures of superconducting proximity structures. A spin-singlet d_{xy}-wave superconductor is infinitely long in the x direction in (a). The width of the superconductor is W in the y direction. The Green's function at a surface is calculated for a semi-infinite superconductor as shown in (b). We attach a normal metal to a superconductor at $x = 0$ in (c), where "cross" symbols represent impurities. A Cooper pair penetrates into the normal metal and causes the proximity effect.

Sec. III, we analyze the chiral property of the surface bound states at zero energy. In Sec. IV, the symmetry of a Cooper pair appearing at a surface of a d_{xy}-wave superconductor with spin-orbit interactions is analyzed by using the anomalous Green's function. In Sec. V, we discuss the anomalous proximity effect when the two types of spin-orbit interaction coexist. The conclusion is given in Sec. VI. In the text of this paper, we use the system of units $\hbar = k_B = c = 1$, where k_B is the Boltzmann constant and c is the speed of light.

II. ANOMALOUS PROXIMITY EFFECT

In this section, we explain the conductance quantization in an NS junction due to the anomalous proximity effect, we provide the necessary conditions for a superconductor exhibiting the anomalous proximity effect, and we illustrate the goals of this paper.

A. Chiral property of ZESs

The most drastic phenomenon of the anomalous proximity effect may be the quantization of the differential conductance in a NS junction shown in Fig. 1(c). The conductance at zero bias can be described by

$$G_{\rm NS} = \frac{2e^2}{h}|\mathcal{N}_{\rm ZES}| \tag{1}$$

in the limit of strong potential disorder in a normal metal, where $|\mathcal{N}_{\rm ZES}|$ represents the number of zero-energy states (ZESs) remaining at a dirty surface of a superconductor [1,5]. We first explain the properties of the index $\mathcal{N}_{\rm ZES}$ in the case of a spin-triplet p_x-wave superconductor, which is an example of a superconductor exhibiting the anomalous proximity effect. At a clean surface of a p_x-wave superconductor, topologically protected bound states appear at zero energy as a result of a nontrivial winding number $\mathcal{W}(k_y) = \pm 1$ in the one-dimensional Brillouin zone [25]. In Fig. 5(a) in Appendix A, we plot the eigenvalues of the BdG Hamiltonian for a p_x-wave superconductor on a two-dimensional tight-binding lattice. The superconducting gap has two nodes at $k_y = \pm k_F$, with $k_F = \pi/2$ being the Fermi wave number. The degree of degeneracy at zero energy is equal to the number of propagating channels on the Fermi surface N_c because each propagating channel $-k_F < k_y < k_F$ accommodates a ZES at a surface. We also show the results for a d_{xy}-wave superconductor in Fig. 5(b). The winding number $\mathcal{W}(k_y)$ can be defined only in the presence of the translational symmetry in the y direction. Therefore, the large degree of degeneracy at zero energy in both Figs. 5(a) and 5(b) is a direct consequence of the translational symmetry of the Hamiltonian in the y direction. The zero-bias conductance in such a ballistic NS junction is described by

$$G_{\rm NS} = \frac{2e^2}{h}N_c. \tag{2}$$

The results are valid for both a p_x-wave junction and a d_{xy}-wave junction.

Random impurities near the surface may lift the degeneracy at zero energy because they break translational symmetry. The index $|\mathcal{N}_{\rm ZES}|$ in Eq. (1) represents the number of the ZESs that remain even in the presence of potential disorder. As discussed in detail later, the index $\mathcal{N}_{\rm ZES}$ can be defined when the Bogoliubov–de Gennes Hamiltonian preserves chiral symmetry. Therefore, we discuss the fundamental symmetries of the BdG Hamiltonian in this paragraph. The BdG Hamiltonian in momentum space is represented as

$$\check{H}_{\rm BdG}(\boldsymbol{k}) = \begin{bmatrix} \hat{H}_{\rm N}(\boldsymbol{k}) & \hat{\Delta}(\boldsymbol{k}) \\ -\hat{\Delta}^*(-\boldsymbol{k}) & -\hat{H}_{\rm N}^*(-\boldsymbol{k}) \end{bmatrix}, \tag{3}$$

where $\hat{H}_{\rm N}(\boldsymbol{k})$ and $\hat{\Delta}(\boldsymbol{k})$ are the normal-state Hamiltonian and the pair potential, respectively. Throughput this paper, the symbols $\check{\cdot}$ and $\hat{\cdot}$ represent 4×4 and 2×2 matrices, respectively. The Hamiltonian for a p_x-wave superconductor in Eq. (A2) preserves time-reversal symmetry,

$$\mathcal{T}_- \check{H}_{\rm BdG} \mathcal{T}_-^{-1} = \check{H}_{\rm BdG}, \quad \mathcal{T}_- = i\hat{\sigma}_2 \mathcal{K}, \tag{4}$$

where $\mathcal{K}$ denotes taking the complex conjugation for a Hamiltonian in real space, and taking the complex conjugation plus applying $\boldsymbol{k} \to -\boldsymbol{k}$ for a Hamiltonian in momentum space. Pauli's matrix in spin space is denoted by $\hat{\sigma}_j$ for $j = 1$–3. A BdG Hamiltonian always preserves particle-hole symmetry,

$$\mathcal{C} \check{H}_{\rm BdG} \mathcal{C}^{-1} = -\check{H}_{\rm BdG}, \quad \mathcal{C} = \hat{\tau}_1 \mathcal{K}, \tag{5}$$

where $\hat{\tau}_j$ for $j = 1$–3 is Pauli's matrix in particle-hole space. By combining the two symmetries, any Hamiltonian belonging to class DIII preserves chiral symmetry,

$$\{\check{\Gamma}_{\rm DIII}, \check{H}_{\rm BdG}\} = 0, \quad \check{\Gamma}_{\rm DIII} = \hat{\tau}_1 \hat{\sigma}_2. \tag{6}$$

Since $\check{\Gamma}_{\rm DIII}^2 = 1$, the eigenvalue of the chiral operator is either 1 or -1. A ZES is always an eigenstate of the chiral operator [25]. Indeed, it is easy to confirm that the Hamiltonian in

Eq. (A2) anticommutes to $\check{\Gamma}_{\rm DIII}$ and that the wave function of surface bound states at zero energy $\phi_{p_x,\pm}$ in Eq. (A5) is the eigenfunction of $\check{\Gamma}_{\rm DIII}$ belonging to the chiral eigenvalue of ± 1. The index in Eq. (1) can be defined by

$$\mathcal{N}_{\rm ZES} \equiv N_+ - N_-, \tag{7}$$

where $N_\pm$ is the number of ZESs belonging to the chiral eigenvalue of ± 1. The index is an invariant as long as the Hamiltonian preserves chiral symmetry in Eq. (6). Thus $\mathcal{N}_{\rm ZES}$ calculated in a clean superconductor remains unchanged even in the presence of potential disorder because the random impurity potential $V_{\rm imp}(\boldsymbol{r})\,\hat{\tau}_3$ preservers the chiral symmetry in Eq. (6). The anomalous proximity effect happens when the index takes a nontrivial value $\mathcal{N}_{\rm ZES} \neq 0$. However, ZESs of $H_{\rm BdG}$ in class DIII always satisfy $\mathcal{N}_{\rm ZES} = 0$ in terms of their chiral eigenvalues of $\check{\Gamma}_{\rm DIII}$ [26]. Therefore, the BdG Hamiltonian of a superconductor exhibiting the anomalous proximity effect must satisfy the following necessary conditions:

(i) $H_{\rm BdG}$ anticommutes to an extra chiral operator other than $\check{\Gamma}_{\rm DIII}$.

(ii) Zero-energy states at the surface of a superconductor have a chiral property such as $\mathcal{N}_{\rm ZES} \neq 0$ in terms of the extra chiral operator.

We show a simple way to find an extra chiral operator as follows. The Hamiltonian in Eq. (A2) remains unchanged under the rotation around the first axis in spin space,

$$\check{R}_1\,\check{H}_{p_x}\,\check{R}_1^{-1} = \check{H}, \quad \check{R}_1 = \hat{\sigma}_1\,\hat{\tau}_3. \tag{8}$$

Using such a spin rotation symmetry, it is possible to define a time-reversal-like symmetry of a Hamiltonian,

$$\mathcal{T}_+\,\check{H}_{p_x}\,\mathcal{T}_+^{-1} = \check{H}_{p_x}, \quad \mathcal{T}_+ = \check{R}_1\mathcal{T}_- = -\hat{\sigma}_3\,\hat{\tau}_3\,\mathcal{K}. \tag{9}$$

As a result of the spin-rotation symmetry of the Hamiltonian, we find

$$\{\check{\Gamma}_{\rm BDI},\, \check{H}_{p_x}\} = 0, \quad \check{\Gamma}_{\rm BDI} = i\mathcal{T}_+\,\mathcal{C} = \hat{\sigma}_3\,\hat{\tau}_2. \tag{10}$$

Since $\mathcal{T}_+^2 = 1$, $\check{H}_{p_x}$ belongs also to class BDI. The wave function of ZESs at the surface of a p_x-wave superconductor can be represented alternatively as $\phi_{p_x,\sigma}$ in Eq. (A6). We find that $\phi_{p_x,\sigma}$ belongs to the positive chiral eigenvalues of $\check{\Gamma}_{\rm BDI}$ irrespective of σ. Therefore, we find $N_+ = N_c$ and $N_- = 0$, which results in $\mathcal{N}_{\rm ZES} = N_c$. A p_x-wave superconductor satisfies the conditions (i) and (ii) in terms of the chiral operator $\check{\Gamma}_{\rm BDI}$. Two of the authors showed that some superconductors under a strong Zeeman field in the presence of spin-orbit interactions preserve such an extra chiral symmetry and host flatband ZESs at their dirty surfaces [26]. The anomalous proximity effect has been considered to be a part of Majorana physics because such artificial superconductors host Majorana fermions at their surface [27,28]. At present, however, we think that a superconductor hosting Majorana fermions is a sufficient condition for the anomalous proximity effect. The necessary conditions (i) and (ii) are more relaxed than those generating Majorana fermions.

B. An odd-frequency s-wave pair

The anomalous proximity effect has two aspects: the penetration of a quasiparticle at zero energy into a dirty metal as discussed in Sec. II A, and the penetration of an odd-frequency Cooper pair into a dirty metal. The existence of $\mathcal{N}_{\rm ZES}$-fold degenerate ZESs can be observed as a large zero-energy peak in the local density of states (LDOS) at a dirty metal. In the mean-field theory of superconductivity, the density of states can be calculated from the normal Green's function $\hat{G}$, and the pairing correlations are described by the anomalous Green's function $\hat{F}$. As the two Green's functions are related to each other through the Gor'kov equation, the enhancement of $\hat{G}$ at zero energy causes an anomaly of $\hat{F}$ at zero energy. The anomalous Green's function in a Matsubara representation $\hat{F}(\boldsymbol{k}, i\omega_n)$ enables us to analyze symmetry of pairing correlations, where $\omega_n = (2n+1)\pi T$ is a fermionic Matsubara frequency and T is a temperature. The anomalous Green's function obeys the antisymmetric relation under the permutation of two electrons consisting of a Cooper pair,

$$\hat{F}^{\rm T}(-\boldsymbol{k}, -i\omega_n) = -\hat{F}(\boldsymbol{k}, i\omega_n), \tag{11}$$

where T means the transpose of a matrix. In the standard representation, the anomalous Green's function is decomposed into four spin components as

$$\hat{F}(\boldsymbol{k}, i\omega_n) = i[f_0(\boldsymbol{k}, i\omega_n) + \boldsymbol{f}(\boldsymbol{k}, i\omega_n)\cdot\hat{\boldsymbol{\sigma}}]\hat{\sigma}_2, \tag{12}$$

where f_0 is a spin-singlet component and $\boldsymbol{f}$ represents three spin-triplet components. In a dirty normal, the diffusive motion of a quasiparticle causes the Green's function to be isotropic in momentum space as

$$\hat{F}(i\omega_n) = i[f_0(i\omega_n) + \boldsymbol{f}(i\omega_n)\cdot\hat{\boldsymbol{\sigma}}]\hat{\sigma}_2. \tag{13}$$

The relation in Eq. (11) implies that the spin-singlet component is an even function of ω_n as $f_0(-i\omega_n) = f_0(i\omega_n)$. The spin-triplet components, on the other hand, are odd functions of ω_n as $\boldsymbol{f}(-i\omega_n) = -\boldsymbol{f}(i\omega_n)$. To compensate for the anomaly of $\hat{G}$ at $\omega_n \to 0$, the anomalous Green's function must have a component of $\hat{F}(i\omega_n) \propto 1/\omega_n$ [29]. Such an odd-frequency pair must be a spin-triplet. Thus the last necessary condition for the anomalous proximity effect is as follows:

(iii) An odd-frequency spin-triplet s-wave pairing correlation $\boldsymbol{f} \propto 1/\omega_n$ exists at the surface as a result of the large zero-energy peak in the local density of states.

In a spin-singlet d_{xy}-wave superconductor, however, no spin-triplet pairing correlation exists in the absence of spin-dependent potentials.

C. Goals of this paper

To clarify one of the motivations of this study, we show that a spin-singlet d_{xy}-wave superconductor without spin-orbit interaction does not cause the anomalous proximity effect. A spin-singlet d_{xy}-wave pair potential is defined by

$$\hat{\Delta}(\boldsymbol{k}) = \Delta_{\boldsymbol{k}}\, i\hat{\sigma}_2, \quad \Delta_{\boldsymbol{k}} = \Delta\,\bar{k}_x\bar{k}_y, \tag{14}$$

where $k_x(k_y)$ is the wave number in the $x(y)$ direction. The wave numbers in the pair potential are normalized to the Fermi wave number k_F as $\bar{k}_x = k_x/k_F$ and $\bar{k}_y = k_y/k_F$. It is easy to confirm that the Hamiltonian for a d_{xy}-wave superconductor in Eq. (A7) anticommutes to $\check{\Gamma}_{\rm BDI}$, and that the wave function of the ZESs at the surface of a d_{xy}-wave superconductor is given in Eq. (A9). Their chiral eigenvalues depend on $\mathrm{sgn}(k_y)$ reflecting the sign change of the pair potential at $k_y = 0$. As

displayed in Fig. 5(b), the number of ZESs at $k_y > 0$ is equal to that at $k_y < 0$. Although Eq. (A7) satisfies condition (i), the index $\mathcal{N}_{\rm ZES}$ is always zero in the absence of spin-orbit interactions. Therefore, we concluded that the random impurity potential completely lifts the high degeneracy at zero energy in Fig. 5(b) and that a d_{xy}-wave superconductor does not show the proximity effect in the absence of spin-dependent potentials.

In the presence of Rashba spin-orbit interaction in a d_{xy}-wave superconductor, the numerical results of the LDOS and those of the pairing correlation in a dirty metal indicate that condition (iii) may be satisfied [11]. The BdG Hamiltonian in momentum space reads

$$\check{H}_0 = (\xi_{\boldsymbol{k}} - \lambda k_x \hat{\sigma}_2)\,\hat{\tau}_3 + \lambda k_y \hat{\sigma}_1 - \Delta_{\boldsymbol{k}} \hat{\tau}_2\,\hat{\sigma}_2, \tag{15}$$

where $\xi_{\boldsymbol{k}} = \boldsymbol{k}^2/2m - \epsilon_F$ is the kinetic energy of a quasiparticle measured from the Fermi energy $\epsilon_F = k_F^2/(2m)$, and λ represents the strength of the spin-orbit interaction. When the two spin-orbit interaction terms $-\lambda k_x \hat{\sigma}_2\,\hat{\tau}_3$ and $\lambda k_y \hat{\sigma}_1$ coexist, $\check{\Gamma}_{\rm DIII}$ is the only chiral operator that anticommutes to $\check{H}_0$. Since $\mathcal{N}_{\rm ZES} = 0$ in terms of the chiral eigenvalues of $\check{\Gamma}_{\rm DIII}$, the degeneracy of the ZESs is fragile in the presence of potential disorder [26]. Thus we infer that the anomalous proximity effect in such a junction would be very weak. Namely, the zero-bias conductance in an NS junction would not be quantized, and the zero-energy peak in the LDOS would disappear in the limit of strong potential disorder.

In such a situation, the goal of this paper is to clarify the roles of the spin-orbit interaction terms in the anomalous proximity effect. To achieve that objective, we analyze the chiral property of the surface bound states of two different superconductors: the Hamiltonian of one superconductor contains only a spin-orbit interaction $\lambda k_y \hat{\sigma}_1$, and that of the other contains only $-\lambda k_x \hat{\sigma}_2\,\hat{\tau}_3$. After showing whether $\mathcal{N}_{\rm ZES}$ is 0 or not for the two superconductors, we make clear how an odd-frequency spin-triplet s-wave pair appears at the surface. On the basis of the obtained results, we provide a theoretical design of a superconductor that exhibits the strong anomalous proximity effect.

III. TWO TYPES OF SUPERCONDUCTOR

We divide the Rashba spin-orbit interaction into two parts $\lambda k_y \hat{\sigma}_1$ and $-\lambda k_x \hat{\sigma}_2\,\hat{\tau}_3$ to study how they modify independently the chiral properties of zero-energy states and the symmetry of a Cooper pair at the surface. Figure 1 shows the schematic pictures of the superconductor under consideration. A superconductor in Fig. 1(a) is infinitely long in the x direction, and the width of the superconductor is W in the y direction. We apply the periodic boundary condition in the y direction. In what follows, we analyze the two BdG Hamiltonians given by

$$\check{H}_1 = \xi_{\boldsymbol{k}} \hat{\tau}_3 + \lambda k_y \hat{\sigma}_1 - \Delta_{\boldsymbol{k}} \hat{\tau}_2\,\hat{\sigma}_2 \tag{16}$$

and

$$\check{H}_2 = \xi_{\boldsymbol{k}} \hat{\tau}_3 - \lambda k_x \hat{\sigma}_2 \hat{\tau}_3 - \Delta_{\boldsymbol{k}} \hat{\tau}_2\,\hat{\sigma}_2. \tag{17}$$

We assume the relation

$$\Delta \ll \lambda k_F \ll \epsilon_F, \tag{18}$$

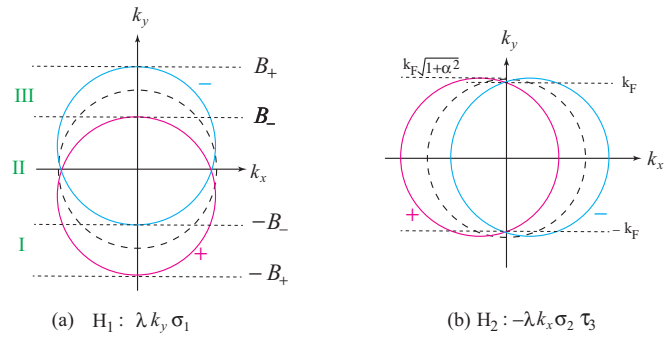

FIG. 2. The two Fermi surfaces for H_1 and those for H_2 are illustrated in (a) and (b), respectively. In (a), the lower (upper) circle indicated by "+" ("−") represents a Fermi surface calculated from $\xi_{1,+}(\boldsymbol{k}) = 0$ [$\xi_{1,-}(\boldsymbol{k}) = 0$]. In (b), the left (right) circle represents a Fermi surface calculated from $\xi_{2,+}(\boldsymbol{k}) = 0$ [$\xi_{2,-}(\boldsymbol{k}) = 0$].

and we discuss the effects of the spin-orbit interaction on the superconducting states within the first order of

$$\alpha \equiv \frac{\lambda k_F}{2\epsilon_F} \ll 1. \tag{19}$$

The main purpose of the next two subsections is to examine whether the two Hamiltonians preserve extra chiral symmetry, and to calculate the index $\mathcal{N}_{\rm ZES}$. In addition, we also define the wave number on the Fermi surface and the number of propagating channels N_c, which are necessary items to represent the anomalous Green's function in Sec. IV.

A. Surface bound states of $\check{H}_1$

We first focus on the $\check{H}_1$ in Eq. (16). The positive eigenvalues of $\check{H}_1$ are calculated to be

$$E_{1,\pm} = \sqrt{\xi_{1,\pm}^2 + \Delta_{\boldsymbol{k}}^2}, \quad \xi_{1,\pm}(k, k_y) = \xi_{\boldsymbol{k}} \pm \lambda k_y. \tag{20}$$

The two Fermi surfaces characterized by $\xi_{1,\pm} = 0$ are illustrated in Fig. 2(a). A wave number in the y direction k_y indicates a transport channel. As shown in Fig. 2(a), the k_y axis is divided into three regions: (I) $-B_+ \leqslant k_y \leqslant -B_-$, (II) $-B_- \leqslant k_y \leqslant B_-$, and (III) $B_- \leqslant k_y \leqslant B_+$, with $B_\pm = [\sqrt{1+\alpha^2} \pm \alpha]k_F$. The wave numbers in the x direction are calculated as

$$p_{1\pm} \equiv \left[k_F^2 - k_y^2 \mp 2\alpha k_y k_F\right]^{1/2}, \tag{21}$$

as a function of k_y. A transport channel at k_y on the Fermi surface of the $\pm$ branch is propagating for $p_{1\pm}^2 > 0$ and is evanescent for $p_{1\pm}^2 < 0$. Therefore,

$$n_+(k_y) \equiv \Theta\left(p_{1+}^2\right) + \Theta\left(p_{1-}^2\right) \tag{22}$$

represents the number of propagating channels at k_y, where $\Theta(x)$ is the step function. We also define

$$n_-(k_y) \equiv \Theta\left(p_{1+}^2\right) - \Theta\left(p_{1-}^2\right) \tag{23}$$

for later use. In Figs. 3(a) and 3(b), we plot $n_\pm$ as a function of k_y. As shown in Fig. 3(a), both $\pm$ branches are propagating in (II) in Fig. 2(a), whereas only one branch is propagating in (I) and (III) in Fig. 2(a). The number of propagating channels

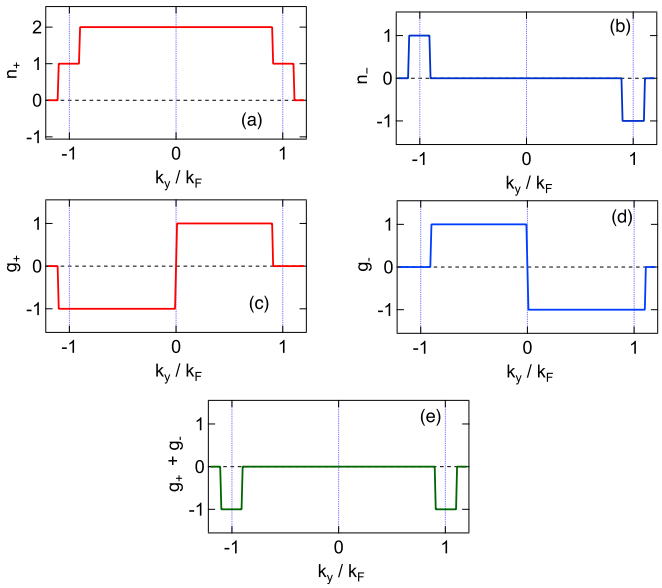

FIG. 3. In (a), $n_+(k_y)$ represents the number of propagating channels at k_y. $n_-(k_y)$ in (b) is an odd function of k_y. The chiral eigenvalues of the ZESs g_+ and g_- are plotted in (c) and (d), respectively. In (e), the summation of the chiral eigenvalues $g_+ + g_-$ is shown. $n_-(k_y)$ in (b) and $g_+ + g_-$ in (e) are nonzero at (I) and (III) in Fig. 2(a).

is calculated as

$$N_c \equiv \sum_{k_y} n_+(k_y) = \frac{W}{2\pi}\int_{-\infty}^{\infty} dk_y\, n_+(k_y), \tag{24}$$

$$= \left[\frac{2Wk_F}{\pi}\right]_{\rm G}, \tag{25}$$

where $[\cdots]_{\rm G}$ is Gauss's symbol, meaning the integer part of the argument. Since a propagating channel hosts a ZES, the number of ZESs at a surface is N_c. A superconductor described by H_1 hosts highly degenerate ZESs at its surface around $x \gtrsim 0$ in Fig. 1(b). As shown in Fig. 3(b), n_- is an odd function of k_y. We use this property when we describe an induced pairing correlation by a spin-orbit interaction in Sec. IV A.

The wave functions of surface bound states at zero energy are described by

$$\psi_{1+}(x) = \begin{bmatrix} 1 \\ 1 \\ is_k \\ -is_k \end{bmatrix} e^{-q_x x} \sin p_{1+}x, \tag{26}$$

$$\psi_{1-}(x) = \begin{bmatrix} -1 \\ 1 \\ is_k \\ is_k \end{bmatrix} e^{-q_x x} \sin p_{1-}x, \tag{27}$$

$$s_k = \mathrm{sgn}(k_y). \tag{28}$$

Here the wave number in the superconducting state is given approximately by

$$\left[p_{1s}^2 \pm 2m\Delta|\bar{p}_{1s}\bar{k}_y|\right]^{1/2} \approx p_{1s} \pm iq_x \tag{29}$$

for $s = \pm$. The imaginary part of the wave number is estimated at $\epsilon = 0$ as $q_x = (\Delta/v_F)|\bar{k}_y|$, with $v_F = k_F/m$ being the Fermi velocity. As shown in Eqs. (26) and (27), q_x characterizes the spatial area of the surface bound states. The Hamiltonian Eq. (16) anticommutes to the extra chiral operator $\check{\Gamma}_{\rm BDI}$ in Eq. (10). It is easy to show that

$$\check{\Gamma}_{\rm BDI}\,\psi_{1\pm} = g_\pm \psi_{1\pm}, \quad g_\pm = \pm s_k. \tag{30}$$

The chiral eigenvalues g_+, g_-, and $g_+ + g_-$ are plotted as a function of k_y in Figs. 3(c), 3(d), and 3(e), respectively. By reflecting the sign change of the pair potential, both g_+ and g_- change their signs at $k_y = 0$ as shown in Figs. 3(c) and 3(d). The index in the terms of the chiral eigenvalue of $\check{\Gamma}_{\rm BDI}$ can be calculated as

$$\mathcal{N}_{\rm ZES} = \sum_{k_y}[g_+ + g_-] = \left[-\frac{2Wk_F}{\pi}\alpha\right]_{\rm G}. \tag{31}$$

The index is a finite value in the presence of spin-orbit interaction. Thus, we conclude that $\check{H}_1$ satisfies the necessary conditions (i) and (ii) in Sec. II A. The zero-bias conductance in a dirty NS junction in Fig. 1(c) can be quantized as Eq. (1). The shift of the Fermi surface by the spin-orbit interaction in Fig. 2(a) causes the index to be a nonzero value because the integrand of Eq. (31) is nonzero at (I) and (III) in Fig. 2(a). Therefore, we will clarify what happens on the anomalous Green's function in these regions in Sec. IV.

B. Surface bound states of $\check{H}_2$

Next, we focus on $\check{H}_2$ in Eq. (17). The positive eigenvalues of $\check{H}_2$ are calculated to be

$$E_{2,\pm} = \sqrt{\xi_{2,\pm}^2 + \Delta_{\boldsymbol{k}}^2}, \quad \xi_{2,\pm}(k, k_y) = \xi_{\boldsymbol{k}} \pm \lambda\, k. \tag{32}$$

In Fig. 2(b), we illustrate the two splitting Fermi surfaces characterized by $\xi_{2,\pm} = 0$. The wave numbers in the x direction on the Fermi surface are calculated as

$$p_{2\pm} = \sqrt{k_F^2 - k_y^2} \mp \alpha k_F. \tag{33}$$

For $|k_y| \leqslant k_F$, the transport channels are propagating. A topologically protected ZES appears for each propagating channel. The wave functions of such surface bound states are calculated as

$$\psi_{2+}(x) = \begin{bmatrix} s_k \\ -is_k \\ 1 \\ -i \end{bmatrix} e^{-q_x x} \sin p_{2+}x, \tag{34}$$

$$\psi_{2-}(x) = \begin{bmatrix} s_k \\ is_k \\ -1 \\ -i \end{bmatrix} e^{-q_x x} \sin p_{2-}x. \tag{35}$$

The Hamiltonian $\check{H}_2$ anticommutes to an extra chiral operator $\hat{\tau}_1$, which is derived from the invariance of $\check{H}_2$ under the rotation about the second axis in spin space $\hat{\sigma}_2\,\hat{\tau}_0$. It is easy to show that $\hat{\tau}_1\,\psi_{2\pm} = \pm s_k\,\phi_{2\pm}$. We find $\mathcal{N}_{\rm ZES} = 0$ because the chiral eigenvalues depend on $\mathrm{sgn}(k_y)$. Namely, $\check{H}_2$ does not satisfy the necessary condition for the anomalous proximity

effect (ii) in Sec. II A. Thus we conclude that the superconductor described by $\check{H}_2$ does not exhibit the anomalous proximity effect because the random impurity potential at its surface lifts the degeneracy at zero energy.

IV. PAIRING CORRELATIONS AT A SURFACE

The purpose of this section is to examine the close relationship between conditions (ii) and (iii) discussed in Sec. II. As $\check{H}_1$ satisfies condition (ii), an odd-frequency spin-triplet s-wave pairing correlation is expected to appear at the surface of a superconductor. We will clarify mechanisms necessary to generate such an odd-frequency pair. As $\check{H}_2$ does not satisfy (ii), we will confirm that an odd-frequency spin-triplet s-wave pairing correlation is absent at its surface.

To this end, we calculate the Green's function at the surface of a superconductor as shown in Fig. 1(b). The outline of the derivation is as follows. We first solve the Gor'kov equation for the retarded Green's function,

$$[\epsilon + i\delta - \check{H}_{\rm BdG}(\boldsymbol{k})]\,\check{G}_\epsilon(\boldsymbol{k}) = \hat{\tau}_0\,\hat{\sigma}_0, \tag{36}$$

$$\check{G}_\epsilon(\boldsymbol{k}) = \begin{bmatrix} \hat{G}_\epsilon(\boldsymbol{k}) & \hat{F}_\epsilon(\boldsymbol{k}) \\ -\hat{F}_\epsilon(\boldsymbol{k}) & -\hat{G}_\epsilon(\boldsymbol{k}) \end{bmatrix}, \tag{37}$$

where $i\delta$ is a small imaginary part of the energy. The "under-tilded" function is defined by

$$\underset{\sim}{X}_\epsilon(\boldsymbol{k}) \equiv X^*_{-\epsilon}(-\boldsymbol{k}), \tag{38}$$

where X is an arbitrary function. Secondly, we calculate the Green's function in real space,

$$\check{G}(\boldsymbol{r},\boldsymbol{r}') = \int_{-\infty}^{\infty} \frac{dk}{2\pi} e^{ik(x-x')} \sum_{k_y} \frac{e^{ik_y(y-y')}}{W}\,\check{G}(\boldsymbol{k}). \tag{39}$$

for an infinitely long superconductor in the x direction as shown in Fig. 1(a). Finally, we introduce a high potential barrier $V\delta(x)\,\hat{\tau}_3$ to divide the infinitely long superconductor into two semi-infinitely long superconductors. One of them is illustrated in Fig. 1(b). The Green's function at the surface $\check{G}^{\rm S}(\boldsymbol{r},\boldsymbol{r}')$ can be calculated by solving the Lippmann-Schwinger equation exactly as explained in Appendix C. The Green's function at a semi-infinite superconductor $\check{\mathbb{G}}$ is represented as

$$\check{\mathbb{G}}(\boldsymbol{r},\boldsymbol{r}') = \check{G}(\boldsymbol{r},\boldsymbol{r}') + \check{G}^{\rm S}(\boldsymbol{r},\boldsymbol{r}'). \tag{40}$$

In the text, we will show only the results of the calculation; the details of the derivation are given in Appendix B.

A. Pairing correlations of $\check{H}_1$

We first study the pairing correlations at the surface of a superconductor described by $\check{H}_1$. The resulting anomalous Green's function at the surface is given by

$$\hat{F}^{\rm S}_{i\omega_n}(\boldsymbol{r},\boldsymbol{r}') = \frac{1}{W}\sum_{k_y} \frac{e^{ik_y(y-y')}}{2\,v_F} e^{-q_x(x+x')} \Bigg[\frac{i}{\Omega_n}\,\sin p_x(x-x')\,\Delta\,\bar{k}_y\,n_+(k_y) - \frac{i}{\Omega_n}\sin p_x(x-x')\,\Delta\,\bar{k}_y\,n_-(k_y)\,\hat{\sigma}_1$$
$$+ \frac{2}{\omega_n}\sin p_x x\,\sin p_x x'\,\Delta\,\bar{k}_y\,n_+(k_y) - \frac{2}{\omega_n}\sin p_x x\,\sin p_x x'\,\Delta\,\bar{k}_y\,n_-(k_y)\,\hat{\sigma}_1 \Bigg] i\hat{\sigma}_2, \tag{41}$$

where $\Omega_n = \sqrt{\omega_n^2 + \Delta_{\hat{k}}^2}$, $p_x = \sqrt{k_F^2 - k_y^2 + 2\alpha|k_y|k_F}$, and we applied the analytic continuation $\epsilon + i\delta \to i\omega_n$ to analyze the symmetry of pairing correlations. We use the standard expression in Eq. (12) to decompose the anomalous Green's function into four spin components. The first term in Eq. (41) represents a spin-singlet d_{xy}-wave pairing correlation because it changes sign under $x \leftrightarrow x'$ and $y \leftrightarrow y'$ independently. Such a pairing correlation is linked to the pair potential in the presence of attractive interactions between two electrons. The third term represents the pairing correlation belonging to an odd-frequency spin-singlet p_y-wave symmetry class. This correlation function changes sign under $y \leftrightarrow y'$, whereas its sign is preserved under $x \leftrightarrow x'$. The spin-singlet d_{xy}-wave component in the anomalous Green's function is an odd function of $x - x'$, which is responsible for two phenomena at the surface: the appearance of highly degenerate bound states at zero energy, and the appearance of an odd-frequency p_y-wave pairing correlation. The first and third terms in Eq. (41) exist even in the absence of spin-orbit interactions. The spin-orbit interaction in $\check{H}_1$ generates a spin-triplet p_x-wave symmetry at the second term from a spin-singlet d_{xy}-wave pairing correlation.

It is easy to confirm that the second term remains unchanged under $y \leftrightarrow y'$ and changes sign under $x \leftrightarrow x'$. In addition, the third term corresponds to an equal spin pairing correlation in the standard expression in Eq. (12). The anomalous Green's function in an infinitely long superconductor consists of two pairing correlations. One belongs to a spin-singlet d_{xy}-wave symmetry. The other belongs to a spin-triplet p_x-wave symmetry as shown in Eq. (B17). Since the spin-triplet p_x-wave pairing correlation is also an odd function of $x - x'$, it induces a subdominant pairing correlation at a surface, as shown in the last term of Eq. (41). The relations among the four components are illustrated schematically in Fig. 4(a). The last pairing correlation in Eq. (41) belongs to an odd-frequency spin-triplet s-wave symmetry. It is easy to check that this component does not change sign in $x \leftrightarrow x'$ and $y \leftrightarrow y'$ independently. As shown in $n_-(k_y)$ in Fig. 3(b), this odd-frequency correlation is nonzero at regions (I) and (III) in Fig. 2(a). This property is closely related to the fact that $g_+ + g_-$ in Eq. (31) is a nonzero value of -1 at these regions as shown in Fig. 3(e). We conclude that spin-orbit interaction in $\check{H}_1$ generates an odd-frequency spin-triplet s-wave pairing correlation at a surface. Thus a superconductor described by $\check{H}_1$

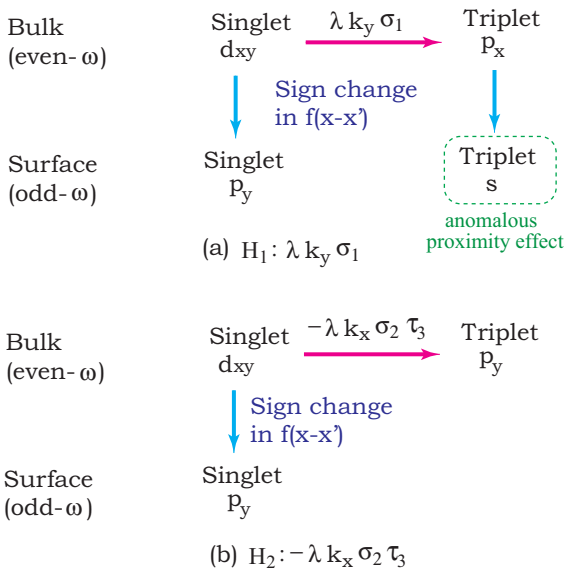

FIG. 4. The pairing correlations appearing in a d_{xy}-wave superconductor. At the surface of a d_{xy}-wave superconductor, an odd-frequency spin-singlet p_y-wave pairing correlation always appears as a result of the sign change in the d_{xy}-wave pairing correlation under $x \leftrightarrow x'$. In (a), a spin-orbit interaction $\lambda k_y \hat{\sigma}_1$ induces spin-triplet p_x-wave pairing correlation in bulk. An odd-frequency spin-triplet s-wave component appears at the surface as a result of the sign change of the p_x-wave pairing correlation. In (b), $-\lambda k_x \hat{\sigma}_2 \hat{\tau}_3$ induces a spin-triplet p_y-wave pairing correlation in bulk, while this interaction does not generate an odd-frequency spin-triplet s-wave correlation at the surface.

also satisfies the last necessary condition (iii) for the anomalous proximity effect.

The local density of states at a surface is calculated from the normal Green's function as

$$N_S(x,\epsilon) \equiv -\frac{1}{2\pi}\mathrm{Im}\int_{-W/2}^{W/2} dy\, \mathrm{Tr}\big[\check{G}^S_\epsilon(\boldsymbol{r},\boldsymbol{r})\big]. \tag{42}$$

The calculated results of the normal Green's function at a surface are given by

$$\hat{G}^S_\epsilon(\boldsymbol{r},\boldsymbol{r}') = \sum_{k_y} \frac{i\, e^{ik_y(y-y')} e^{-q_x(x+x')}}{2W v_{p_x}\Omega}\Bigg[\epsilon\cos p_x(x+x') + i\,\Omega\,\sin p_x(x+x') + 2\frac{\Delta^2_{\hat{\boldsymbol{k}}}}{\epsilon+i\delta}\,\sin p_x x\,\sin p_x x'\Bigg] \times [n_+(k_y) + n_-(k_y)\,\hat{\sigma}_1]. \tag{43}$$

The LDOS at a surface results in

$$N_S(x,\epsilon) = \delta(\epsilon)\sum_{k_y}\frac{2|\Delta_{\boldsymbol{k}}|}{v_{p_x}}\{\sin(p_x x)e^{-q_x x}\}^2 n_+(k_y) \tag{44}$$

for $\epsilon \ll \Delta$. The local density of states at a surface has a peak at zero energy, which reflects the presence of highly degenerate surface bound states at zero energy. The appearance of an odd-frequency pairing correlation and that of surface bound states at zero energy are linked to each other directly. Mathematically, $\epsilon + i\delta$ in the denominator of $\hat{G}^S$ in Eq. (43) and ω_n in the denominator of the odd-frequency components of $\hat{F}^S$ in Eq. (41) have the same origin within the analytic continuation $\epsilon + i\delta \to i\omega_n$. The transformation of

$$\frac{1}{\epsilon+i\delta} = \frac{P}{\epsilon} - i\pi\delta(\epsilon) \tag{45}$$

implies that the zero-energy peak in the LDOS is a consequence of the appearance of an odd-frequency Cooper pair at a surface.

B. Pairing correlations of $\check{H}_2$

The Green's function of a superconductor described by $\check{H}_2$ is also calculated by solving the Lippmann-Schwinger equation. The anomalous Green's function at a surface results in

$$F^S_{i\omega_n}(\boldsymbol{r},\boldsymbol{r}') = \frac{1}{W}\sum_{k_y} e^{ik_y(y-y')}\frac{e^{-q_x(x+x')}}{v_x} \times\Bigg[i\frac{\Delta_{\boldsymbol{k}}}{\Omega_n}\sin k_x(x-x') + \frac{2}{\omega_n}\Delta_{\boldsymbol{k}}\,\sin k_x x\,\sin k_x x' + \frac{\alpha\,\Delta\,\bar{k}_y}{\Omega_n}\cos k_x(x-x')\,\hat{\sigma}_2\Bigg] i\,\hat{\sigma}_2. \tag{46}$$

The first term belongs to spin-singlet d_{xy}-wave symmetry and is linked to the pair potential. The second term is induced at the surface and belongs to odd-frequency spin-singlet p_y-wave symmetry. Due to breaking local inversion symmetry at the surface, a spin-singlet p_y-wave component is generated from a spin-singlet d_{xy}-wave pairing correlation. As already discussed in Eq. (41), these two correlations exist in the absence of spin-orbit interactions. The spin-orbit interaction in $\check{H}_2$ generates a spin-triplet p_y-wave symmetry pairing correlation at the third term, which changes sign under $y \leftrightarrow y'$ but retains its sign under $x \leftrightarrow x'$. The relations among the pairing correlations are illustrated in Fig. 4(b). In Eq. (46), however, an odd-frequency spin-triplet s-wave correlation is absent, as we expected at the beginning of this section. The usual proximity effect is also absent in a normal metal attached to a superconductor because all of the pairing correlations in Eq. (46) are odd functions of $y - y'$ [14–16]. Thus the spin-orbit interaction $\lambda k_x \hat{\sigma}_2\,\hat{\tau}_3$ does not contribute to the proximity effect.

V. DISCUSSION

We have concluded that a superconductor described by $\check{H}_1$ in Eq. (16) satisfies all the necessary conditions for the anomalous proximity effect. On the other hand, a superconductor described by $\check{H}_2$ in Eq. (17) does not exhibit any type of proximity effect. Here we discuss briefly the proximity effect of a d_{xy}-wave superconductor, where the two spin-orbit interaction terms coexist and form the Rashba spin-orbit interaction $\lambda k_y \hat{\sigma}_1 - \lambda k_x \hat{\sigma}_2\,\hat{\tau}_3$. Unfortunately, the coexistence of the two interaction terms weakens the anomalous proximity effect seriously because the interaction $-\lambda k_x \hat{\sigma}_2\,\hat{\tau}_3$ breaks the extra chiral symmetry of $\check{H}_1$. It is easy to confirm that $-\lambda k_x \hat{\sigma}_2 \hat{\tau}_3$ does not anticommute to Γ_{BDI}. Therefore, a random impurity potential lifts the degeneracy at the zero energy. This explains why the signal of the anomalous proximity effect in Ref. [11]

is very weak. Simultaneously, this discussion will determine the design guidelines for superconductors. We conclude that a d_{xy}-wave superconductor described by $\check{H}_1$ is necessary to observe the strong anomalous proximity effect such as the conductance quantization in a NS junction in Eq. (1) and the fractional current-phase relationship of the Josephson current in an SNS junction.

The control of spin-orbit interactions has been an important issue also in spintronics. The spin-orbit interaction in $\check{H}_1$ can be realized by tuning the Rashba spin-orbit interaction and the Dresselhaus spin-orbit interaction. It has been known that such an interaction stabilizes a specialized spin configuration in momentum space called the persistent spin helix [30–34]. Thus it would be possible to fabricate a superconductor that exhibits the strong anomalous proximity effect by combining existing technologies.

The anomalous proximity effect has been considered as a phenomenon unique to spin-triplet superconductors such as a p_x-wave superconductor in Eq. (A2), a Majorana nanowire [6–9], and two-dimensional artificial spin-triplet superconductors hosting a flat Majorana band at its surface [27,28]. There is no doubt that the existence of a spin-triplet order parameter (pair potential) is a sufficient condition for a superconductor to exhibit the anomalous proximity effect. On the other hand, we conclude that the necessary conditions discussed in Sec. II can be satisfied by a specific spin-triplet pairing correlation on a spin-singlet superconductor. Our results indicate a way of enriching the superconducting properties of high-T_c cuprate superconductors.

VI. CONCLUSION

We theoretically studied the effects of spin-orbit interactions in a spin-singlet d_{xy}-wave superconductor on the symmetry of the pairing correlations and those on the chiral properties of the zero-energy bound states at the surface. The Hamiltonian for a d_{xy}-wave superconductor with a specific spin-orbit interaction preserves chiral symmetry. The chiral property of the surface bound states is analyzed in terms of an index $\mathcal{N}_{\rm ZES}$, which is a measure of the strength of the anomalous proximity effect. Our results show that the spin-orbit interaction modifies the chiral property of the surface bound states drastically. As a result, $\mathcal{N}_{\rm ZES}$ can be nontrivial nonzero values. The symmetry of the pairing correlations at the surface of a superconductor are analyzed by using the anomalous Green's function, which is obtained by solving the Gor'kov equation and the Lippmann-Schwinger equation analytically. The spin-orbit interactions induce spatially uniform spin-triplet p-wave pairing correlations in a d_{xy}-wave superconductor. A p-wave pairing correlation generates an odd-frequency spin-triplet s-wave Cooper pair at the surface of a d_{xy}-wave superconductor. We conclude that the presence of a spin-triplet pairing correlation causes the anomalous proximity effect even when a spin-triplet order parameter is absent.

To assist these conclusions, we should study low-energy transport properties through a dirty normal metal such as the conductance in a NS junction and the Josephson current in a SNS junction. An investigation using numerical simulations is underway, and the results will be presented elsewhere.

ACKNOWLEDGMENTS

The authors are grateful to S. Tamura, Y. Tanaka, and D. Manske for useful discussion. This work was supported by JSPS KAKENHI (No. JP20H01857), JSPS Core-to-Core Program (No. JPJSCCA20170002), and JSPS and Russian Foundation for Basic Research under Japan-Russia Research Cooperative Program Grant No. 19-52-50026.

APPENDIX A: SURFACE ANDREEV BOUND STATES

The BdG Hamiltonian on a two-dimensional tight-binding lattice is represented by

$$\mathcal{H} = \sum_{\boldsymbol{r},\boldsymbol{r}'} [\psi^\dagger_{\boldsymbol{r},\uparrow}, \psi^\dagger_{\boldsymbol{r},\downarrow}, \psi_{\boldsymbol{r},\uparrow}, \psi_{\boldsymbol{r},\downarrow}] \check{H}_{\rm BdG}(\boldsymbol{r},\boldsymbol{r}') \times [\psi_{\boldsymbol{r}',\uparrow}, \psi_{\boldsymbol{r}',\downarrow}, \psi^\dagger_{\boldsymbol{r}',\uparrow}, \psi^\dagger_{\boldsymbol{r}',\downarrow}]^{\rm T}, \tag{A1}$$

where $\psi_{\boldsymbol{r},\sigma}$ is the annihilation operator of an electron at $\boldsymbol{r} = j\hat{\boldsymbol{x}} + m\hat{\boldsymbol{y}}$, with $\hat{\boldsymbol{x}}$ ($\hat{\boldsymbol{y}}$) being a unit vector in the $\boldsymbol{x}$ ($\boldsymbol{y}$) direction, $\sigma = \uparrow$ or $\downarrow$ indicates the spin of an electron, and T represents the transpose of a matrix. The BdG Hamiltonian for an equal spin-triplet p_x-wave superconductor can be represented as

$$\check{H}_{p_x}(\boldsymbol{r},\boldsymbol{r}') = H_t(\boldsymbol{r},\boldsymbol{r}')\hat{\tau}_3 + \hat{H}_{\Delta_p}(\boldsymbol{r},\boldsymbol{r}')\,\hat{\sigma}_3\,\hat{\tau}_1, \tag{A2}$$

$$H_t(\boldsymbol{r},\boldsymbol{r}') = -t[\delta_{\boldsymbol{r},\boldsymbol{r}'+\hat{\boldsymbol{x}}} + \delta_{\boldsymbol{r},\boldsymbol{r}'-\hat{\boldsymbol{x}}} + \delta_{\boldsymbol{r},\boldsymbol{r}'+\hat{\boldsymbol{y}}} + \delta_{\boldsymbol{r},\boldsymbol{r}'-\hat{\boldsymbol{y}}}]\hat{\sigma}_0 + \delta_{\boldsymbol{r},\boldsymbol{r}'}(4t - \epsilon_F)\hat{\sigma}_0, \tag{A3}$$

$$H_{\Delta_p} = \frac{\Delta}{2i}[\delta_{\boldsymbol{r},\boldsymbol{r}'+\hat{\boldsymbol{x}}} - \delta_{\boldsymbol{r},\boldsymbol{r}'-\hat{\boldsymbol{x}}}], \tag{A4}$$

where τ_j and σ_j for $j = 1$–3 are Pauli's matrices in particle-hole space and those in spin space, respectively. The unit matrix in these spaces is $\hat{\tau}_0$ and $\hat{\sigma}_0$. The pair potential and the hopping integral are denoted by Δ and t, respectively. We calculate the eigenvalues of $\hat{H}_{p_x}$ under the hard wall boundary condition in the x direction and the periodic boundary condition in the y direction. The results for $\epsilon_F = 2t$ and $\Delta = t$ are plotted as a function of k_y in Fig. 5(a). The symbols for $E \neq 0$ represent eigenvalues of bulk states. At the present parameter choice, the superconducting gap has two nodes at $k_y = \pm k_F$ with $k_F = \pi/2$. The ZESs between the nodes in Fig. 5(a) are localized at a surface. The wave function of the ZESs near $x = 0$ are described by

$$\phi_{p_x,-}(\boldsymbol{r}) = \begin{bmatrix} 1 \\ 1 \\ i \\ -i \end{bmatrix} f_{k_y}(\boldsymbol{r}), \quad \phi_{p_x,+}(\boldsymbol{r}) = \begin{bmatrix} -1 \\ 1 \\ i \\ i \end{bmatrix} f_{k_y}(\boldsymbol{r}),$$

$$f_{k_y}(\boldsymbol{r}) = A\, e^{ik_y y} e^{-x/\xi_0} \sin k_x x, \tag{A5}$$

where $\xi_0 = v_F/\Delta$, and A is a constant. It is easy to confirm that $\check{\Gamma}_{\rm BIII}\,\phi_\pm = \pm\phi_\pm$. As a result, we find $N_+ = N_-$ and $\mathcal{N}_{\rm ZES} = 0$, in agreement with the prediction [26].

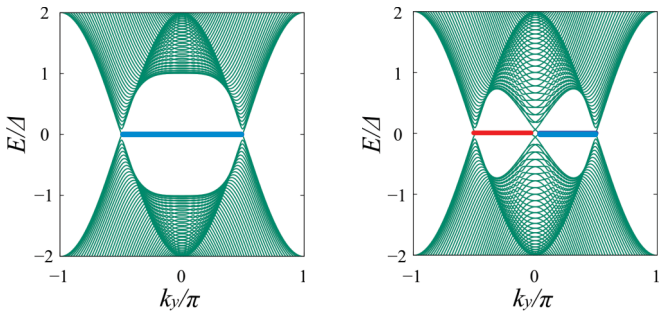

(a) p_x-wave (b) d_{xy}-wave

FIG. 5. The eigenvalues of the BdG Hamiltonian on a two-dimensional tight-binding model are plotted as a function of the wave number in the y direction. The results for a p_x-wave superconductor in (a) have nodes at $k_y = \pm k_F$ with $k_F = \pi/2$. The surface Andreev bound states are degenerate at $E = 0$ as indicated by a line between the two nodal points. All of the ZESs belong to the same chiral eigenvalue of $\check{\Gamma}_{\rm BDI}$. In (b), the results for a d_{xy}-wave superconductor are shown. An additional nodal point appears at $k_y = 0$. ZESs for $k_y > 0$ and those for $k_y < 0$ belong to the opposite chiral eigenvalue of $\check{\Gamma}_{\rm BDI}$.

The wave functions of the ZESs in Eq. (A5) are described alternatively as

$$\phi_{p_x,\uparrow}(\boldsymbol{r}) = \begin{bmatrix} 1 \\ 0 \\ i \\ 0 \end{bmatrix} f_{k_y}(\boldsymbol{r}), \quad \phi_{p_x,\downarrow}(\boldsymbol{r}) = \begin{bmatrix} 0 \\ 1 \\ 0 \\ -i \end{bmatrix} f_{k_y}(\boldsymbol{r}), \tag{A6}$$

where $\phi_{p_x,\sigma}$ is the wave function in the spin σ sector. It is easy to confirm that $\check{\Gamma}_{\rm BDI}\,\phi_\sigma = \phi_\sigma$ holds for both $\sigma = \uparrow$ and $\downarrow$. Therefore, we find $N_+ = N_c$ and $N_- = 0$, which results in $\mathcal{N}_{\rm ZES} = N_c$ as long as $\{\check{H}_{p_x}, \check{\Gamma}_{\rm BDI}\} = 0$.

The eigenvalues of the BdG Hamiltonian of a d_{xy}-wave superconductor,

$$\check{H}_{d_{xy}}(\boldsymbol{r},\boldsymbol{r}') = H_t(\boldsymbol{r},\boldsymbol{r}')\hat{\tau}_3 + H_{\Delta_d}(\boldsymbol{r},\boldsymbol{r}')\,\hat{\sigma}_2\,\hat{\tau}_2, \tag{A7}$$

$$H_{\Delta_d}(\boldsymbol{r},\boldsymbol{r}') = \frac{\Delta}{2}[\delta_{\boldsymbol{r},\boldsymbol{r}'+\hat{x}+\hat{y}} + \delta_{\boldsymbol{r},\boldsymbol{r}'-\hat{x}-\hat{y}} - \delta_{\boldsymbol{r},\boldsymbol{r}'+\hat{x}-\hat{y}} - \delta_{\boldsymbol{r},\boldsymbol{r}'-\hat{x}+\hat{y}}], \tag{A8}$$

are shown in Fig. 5(b). There are three nodal points at $k_y = 0$ and $\pm k_F$. A surface Andreev bound state appears for each propagating channel on the Fermi surface. The wave functions of the ZESs are described by

$$\phi_{d_{xy},+}(\boldsymbol{r}) = \begin{bmatrix} 1 \\ -1 \\ i\,s_k \\ i\,s_k \end{bmatrix} f_{k_y}(\boldsymbol{r}), \quad \phi_{d_{xy},-}(\boldsymbol{r}) = \begin{bmatrix} 1 \\ 1 \\ -i\,s_k \\ i\,s_k \end{bmatrix} f_{k_y}(\boldsymbol{r}),$$
$$s_k = \mathrm{sgn}(k_y). \tag{A9}$$

It is easy to confirm that $\check{\Gamma}_{\rm BDI}\,\phi_{d_{xy},\pm} = \pm s_k\,\phi_{d_{xy},\pm}$ holds. The chiral eigenvalues of ZESs depend on the sign of k_y in a d_{xy}-wave superconductor. As displayed in Fig. 5(b), the number of ZESs at $k_y > 0$ is equal to that at $k_y < 0$. Although $\check{H}_{d_{xy}}$ anticommutes to $\check{\Gamma}_{\rm BDI}$, the index $\mathcal{N}_{\rm ZES}$ is always zero in the absence of spin-orbit interactions. The Hamiltonian $\check{H}_{d_{xy}}$ anticommutes also to another chiral operator $\hat{\tau}_1$. However, we find that $\mathcal{N}_{\rm ZES} = 0$ in terms of the chiral eigenvalues of $\hat{\tau}_1$.

APPENDIX B: GREEN'S FUNCTION IN REAL SPACE

The solution of the Gor'kov equation in Eq. (36) is obtained as

$$\hat{G}_\epsilon(\boldsymbol{k}) = [(\epsilon - \hat{H}_{\rm N}) + \hat{\Delta}\,(\epsilon + \hat{\tilde{H}}_{\rm N})^{-1}\,\hat{\tilde{\Delta}}]^{-1}, \quad \hat{F}_\epsilon(\boldsymbol{k}) = [\hat{\tilde{\Delta}} + (\epsilon + \hat{\tilde{H}}_{\rm N})\,\hat{\Delta}^{-1}\,(\epsilon - \hat{H}_{\rm N})]^{-1}. \tag{B1}$$

The retarded Green's function for H_1 is represented as

$$\hat{G}_\epsilon(\boldsymbol{r}-\boldsymbol{r}') = \frac{1}{W}\sum_{k_y} e^{ik_y(y-y')}\hat{G}_\epsilon(x-x'), \quad \hat{F}_\epsilon(\boldsymbol{r}-\boldsymbol{r}') = \frac{1}{W}\sum_{k_y} e^{ik_y(y-y')}\hat{F}_\epsilon(x-x'), \tag{B2}$$

with

$$\hat{G}_\epsilon(x-x') = \frac{1}{2\pi}\int_{-\infty}^{\infty} dk\, e^{ik(x-x')}\frac{1}{2}\left[\frac{(\epsilon+\xi_{1,+})(1+\hat{\sigma}_1)}{(\epsilon+i\delta)^2 - E_{1,+}^2} + \frac{(\epsilon+\xi_{1,-})(1-\hat{\sigma}_1)}{(\epsilon+i\delta)^2 - E_{1,-}^2}\right], \tag{B3}$$

$$\hat{F}_\epsilon(x-x') = \frac{1}{2\pi}\int_{-\infty}^{\infty} dk\, e^{ik(x-x')}\frac{\Delta_k}{2}\left[\frac{1-\hat{\sigma}_1}{(\epsilon+i\delta)^2 - E_{1,-}^2} + \frac{1+\hat{\sigma}_1}{(\epsilon+i\delta)^2 - E_{1,+}^2}\right] i\hat{\sigma}_2. \tag{B4}$$

To proceed with the calculation, it is necessary to carry out the integration

$$I_{1,\pm} = \frac{1}{2\pi}\int_{-\infty}^{\infty} dk\, e^{ik(x-x')}\,\frac{f(k,\xi_{1,\pm})}{(\epsilon+i\delta-E_{1,\pm})(\epsilon+E_{1,\pm})}, \tag{B5}$$

where f is an analytic function. For $\epsilon > 0$, $(\epsilon + E_{1,\pm})^{-1}$ is analytic, whereas $(\epsilon + i\delta - E_{1,\pm})^{-1}$ has two poles at $k = k_\pm^e + i0^+$ and $k = -k_\pm^h + i0^+$ with

$$k_\pm^e = \left[p_{1\pm}^2 + \frac{2m}{\hbar^2}\Omega\right]^{1/2}, \quad k_\pm^h = \left[p_{1\pm}^2 - \frac{2m}{\hbar^2}\Omega\right]^{1/2}, \quad \Omega = \sqrt{(\epsilon+i\delta)^2 - \Delta_{\boldsymbol{k}}^2}, \tag{B6}$$

where $p_{1\pm}$ is defined in Eq. (21). Paying attention to the relations $\xi_{1,\pm} \to \Omega$ at $k = k^e_\pm$ and $\xi_{1,\pm} \to -\Omega$ at $k = -k^h_\pm$, $\epsilon + i\delta - E_{1,\pm}$ at the denominator of Eq. (B5) can be expanded around $k = k^e_\pm$ as

$$\epsilon + i\delta - E_{1,\pm}(k) \approx \epsilon - E_{1,\pm}(k^e_\pm) + i\delta - \frac{\xi_{1,\pm}}{E_{1,\pm}(k^e_\pm)}\frac{\hbar^2 k^e_\pm}{m}(k - k^e_\pm) = -\frac{\Omega}{\epsilon}\frac{\hbar^2 k^e_\pm}{m}(k - k^e_\pm - i\delta'). \tag{B7}$$

Around a pole of $k = -k^h_\pm$, the $\epsilon + i\delta - E_{1,\pm}$ becomes

$$\epsilon + i\delta - E_{1,\pm}(k) \approx \epsilon - E_{1,\pm}(-k^h_\pm) + i\delta - \frac{\xi_{1,\pm}}{E_{1,\pm}(-k^h_\pm)}\frac{-\hbar^2 k^h_\pm}{m}(k + k^h_\pm) = -\frac{-\Omega}{\epsilon}\frac{(-\hbar^2 k^h_\pm)}{m}(k + k^h_\pm - i\delta'). \tag{B8}$$

By picking up the residues of these poles, the integral in Eq. (B5) is calculated as

$$I_{1,\pm} = -i\frac{m}{2\Omega\hbar^2}\left[\frac{f(s_x k^e_\pm, \Omega)}{k^e_\pm}e^{ik^e_\pm|x-x'|} + \frac{f(-s_x k^h_\pm, -\Omega)}{k^e_\pm}e^{-ik^h_\pm|x-x'|}\right]\Theta(p^2_{1\pm}), \tag{B9}$$

$$s_x = \mathrm{sgn}(x - x'), \tag{B10}$$

where we consider the contribution from the propagating channels as indicated by a factor $\Theta(p^2_{1\pm})$. The integral on the upper-half complex plane converges for $x - x' > 0$. On the other hand, for $x - x' < 0$, the transformation of $k \to -k$ is necessary, which produces a factor of s_x. In the text, we mainly discuss the Green's function for $0 < \epsilon \ll \Delta$. In such a case, it is possible to apply an approximation for the wave number $k^e_\pm = p_{1\pm} + iq_x$ and $k^h_\pm = p_{1\pm} - iq_x$ with $q_x = (\Delta/\hbar v_F)\bar{k}_y$. We also apply $p_{1+} \approx p_{1-} \approx p_x = \sqrt{k_F^2 - k_y^2 + 2\alpha k_F|k_y|}$ because the amplitude of the wave number is not important for analyzing the pairing symmetry. For the same reason, we consider q_x only in the exponential function. The integral under these approximations is represented as

$$I_{1,\pm} \approx -i\frac{m}{2\Omega\hbar^2}e^{-q_x|x-x'|}\left[\frac{f(s_x p_x, \Omega)}{p_x}e^{ip_x|x-x'|} + \frac{f(-s_x p_x, -\Omega)}{p_x}e^{-ip_x|x-x'|}\right]\Theta(p^2_{1\pm}). \tag{B11}$$

The normal Green's function in Eq. (B3) is calculated as

$$\begin{aligned} G_\epsilon(x - x') &= -i\frac{m}{4\Omega\hbar^2}e^{-q_x|x-x'|}\left[\frac{\epsilon + \Omega}{p_x}e^{ip_x|x-x'|} + \frac{\epsilon - \Omega}{p_x}e^{-ip_x|x-x'|}\right](1 + \hat{\sigma}_1)\Theta(p^2_{1+}) \\ &\quad - i\frac{m}{4\Omega\hbar^2}e^{-q_x|x-x'|}\left[\frac{\epsilon + \Omega}{p_x}e^{ip_x|x-x'|} + \frac{\epsilon - \Omega}{p_x}e^{-ip_x|x-x'|}\right](1 - \hat{\sigma}_1)\Theta(p^2_{1-}), \qquad \text{(B12)} \\ &= -i\frac{e^{-q_x|x-x'|}}{2\Omega\hbar v_{p_x}}[\epsilon\,\cos(p_x|x - x'|) + i\,\Omega\,\sin(p_x|x - x'|)][n_+(k_y) + n_-(k_y)\hat{\sigma}_1]. \qquad \text{(B13)} \end{aligned}$$

The anomalous Green's function results in

$$\begin{aligned} F_\epsilon(x - x') &= -i\frac{ms_x}{4\Omega\hbar^2}e^{-q_x|x-x'|}\left[\frac{\Delta\bar{k}_y\bar{p}_x}{p_x}e^{ip_x|x-x'|} - \frac{\Delta\bar{k}_y\bar{p}_x}{p_x}e^{-ip_x|x-x'|}\right](1 + \hat{\sigma}_1)\Theta(p^2_{1+})i\hat{\sigma}_2 \\ &\quad - i\frac{ms_x}{4\Omega\hbar^2}e^{-q_x|x-x'|}\left[\frac{\Delta\bar{k}_y\bar{p}_x}{p_x}e^{ip_x|x-x'|} - \frac{\Delta\bar{k}_y\bar{p}_x}{p_x}e^{-ip_x|x-x'|}\right](1 - \hat{\sigma}_1)\Theta(p^2_{1-})\,i\hat{\sigma}_2, \qquad \text{(B14)} \\ &= -i\frac{e^{-q_x|x-x'|}}{2\Omega\hbar v_F}i\Delta\bar{k}_y\sin p_x(x - x')[n_+(k_y) + n_-(k_y)\hat{\sigma}_1]i\hat{\sigma}_2. \qquad \text{(B15)} \end{aligned}$$

To obtain the Green's function at a surface, the four parts of the Green's function in a uniform superconductor are necessary. We supply them as follows:

$$\hat{G}_{i\omega_n}(x - x') = -\frac{m}{2\Omega_n\hbar^2}\frac{e^{-q_x|x-x'|}}{p_x}[i\hbar\omega_n\,\cos(p_x|x - x'|) - \,\Omega_n\,\sin(p_x|x - x'|)][n_+(k_y) + n_-(k_y)\hat{\sigma}_1], \tag{B16}$$

$$\hat{F}_{i\omega_n}(x - x') = -\frac{m}{2\Omega_n\hbar^2}\frac{e^{-q_x|x-x'|}}{p_x}\,\Delta\bar{p}_x\bar{k}_y\,i\sin p_x(x - x')[n_+(k_y) + n_-(k_y)\,\hat{\sigma}_1]i\,\hat{\sigma}_2, \tag{B17}$$

$$-\hat{\tilde{G}}_{i\omega_n}(x - x') = -\frac{m}{2\Omega_n\hbar^2}\frac{e^{-q_x|x-x'|}}{p_x}[i\hbar\omega_n\,\cos(p_x|x - x'|) + \,\Omega_n\,\sin(p_x|x - x'|)][n_+(k_y) - n_-(k_y)\hat{\sigma}_1], \tag{B18}$$

$$-\hat{\tilde{F}}_{i\omega_n}(x - x') = -\frac{m}{2\Omega_n\hbar^2}\frac{e^{-q_x|x-x'|}}{p_x}\,\Delta\bar{p}_x\bar{k}_y\,i\sin p_x(x - x')[-n_+(k_y) + n_-(k_y)\,\hat{\sigma}_1]i\,\hat{\sigma}_2, \tag{B19}$$

where $\Omega_n = \sqrt{(\hbar\omega_n)^2 + \Delta_{\boldsymbol{k}}^2}$ and the particle-hole transformation is expressed by

$$\underset{\sim}{X}_{i\omega_n}(x, k_y) = X^*_{i\omega_n}(x, -k_y) \tag{B20}$$

in this representation.

The solution of the Gor'kov equation for $\check{H}_2$ is represented as

$$\hat{G}_\epsilon(x - x') = \frac{1}{2\pi}\int_{-\infty}^{\infty} dk\, e^{ik(x-x')}\frac{1}{2}\left[\frac{(\epsilon + \xi_{2,+})(1+\hat{\sigma}_2)}{(\epsilon + i\delta)^2 - E_{2,+}^2} + \frac{(\epsilon + \xi_{2,-})(1-\hat{\sigma}_2)}{(\epsilon + i\delta)^2 - E_{2,-}^2}\right], \tag{B21}$$

$$\hat{F}_\epsilon(x - x') = \frac{1}{2\pi}\int_{-\infty}^{\infty} dk\, e^{ik(x-x')}\frac{\Delta_{\boldsymbol{k}}}{2}\left[\frac{1-\hat{\sigma}_2}{(\epsilon + i\delta)^2 - E_{2,-}^2} + \frac{1+\hat{\sigma}_2}{(\epsilon + i\delta)^2 - E_{2,+}^2}\right] i\hat{\sigma}_2. \tag{B22}$$

Within first order α, the retarded Green's functions in an infinitely long superconductor are calculated as

$$\hat{G}_\epsilon(x - x') = \frac{-i}{\Omega\,\hbar v_{k_x}} e^{-q_x|x-x'|}[\epsilon\cos k_x|x - x'| + i\Omega\sin k_x|x - x'|], \tag{B23}$$

$$\hat{F}_\epsilon(x - x') = \frac{-i}{\Omega\,\hbar v_{k_x}} e^{-q_x|x-x'|}[i\Delta_{\boldsymbol{k}}\sin k_x(x - x') + \alpha\,\Delta\,\bar{k}_y\cos k_x(x - x')\hat{\sigma}_2]\, i\hat{\sigma}_2. \tag{B24}$$

Here we apply the relation

$$I_{2,\pm} = \frac{1}{2\pi}\int_{-\infty}^{\infty} dk\, e^{ik(x-x')}\,\frac{f(k, \xi_{2,\pm})}{(\epsilon + i\delta - E_{2,\pm})(\epsilon + E_{2,\pm})}, \tag{B25}$$

$$= -i\frac{e^{-q_x|x-x'|}}{2\Omega\hbar v_x}[f(\mp\alpha k_F + s_x k_x, \Omega)\, e^{ik_x|x-x'|} + f(\mp\alpha k_F - s_x k_x, -\Omega)\, e^{-ik_x|x-x'|}], \tag{B26}$$

where $v_x = \hbar k_x/m$, and $k_x = \sqrt{k_F^2 - k_y^2}$ is a real wave number.

APPENDIX C: LIPPMANN-SCHWINGER EQUATION

The Lippmann-Schwinger equation relates the Green's function in the presence of a perturbation $\check{\mathbb{G}}$ to that in the absence of the perturbation $\check{G}$ as

$$\check{\mathbb{G}}_{i\omega_n}(\boldsymbol{r}, \boldsymbol{r}') = \check{G}_{i\omega_n}(\boldsymbol{r}, \boldsymbol{r}') + \int d\boldsymbol{r}_1\, \check{G}_{i\omega_n}(\boldsymbol{r}, \boldsymbol{r}_1)\check{V}(\boldsymbol{r}_1)\,\check{\mathbb{G}}_{i\omega_n}(\boldsymbol{r}_1, \boldsymbol{r}'), \tag{C1}$$

where $\check{V}(\boldsymbol{r})$ is the perturbation potential. In this paper, we introduce a wall at $x = x_0$,

$$\check{V}(\boldsymbol{r}) = V\,\delta(x - x_0)\,\hat{\tau}_3, \tag{C2}$$

to divide an infinitely long superconductor into two semi-infinite superconductors. Thus $G_{i\omega_n}$ is the Green's function in an infinitely long superconductor in the x direction. Although the wall breaks the translational symmetry in the x direction, the superconductor is translationally invariant in the y direction. Therefore, it is possible to represent the Green's function as

$$\check{\mathbb{G}}_{i\omega_n}(\boldsymbol{r}, \boldsymbol{r}') = \frac{1}{W}\sum_{k_y}\check{\mathbb{G}}_{i\omega_n}(x, x')e^{ik_y(y-y')}. \tag{C3}$$

By substituting the expression into the equation, we find

$$\check{\mathbb{G}}_{i\omega_n}(x, x') = \check{G}_{i\omega_n}(x, x') + \check{G}_{i\omega_n}(x, x_0)\,V\hat{\tau}_3\,\check{\mathbb{G}}_{i\omega_n}(x_0, x'). \tag{C4}$$

By setting $x = x_0$, we obtain the Green's function

$$\check{\mathbb{G}}_{i\omega_n}(x_0, x') = [1 - \check{G}_{i\omega_n}(x_0, x_0)\,V\,\hat{\tau}_3]^{-1}\check{G}_{i\omega_n}(x_0, x'). \tag{C5}$$

Finally, we obtain the relations

$$\check{\mathbb{G}}_{i\omega_n}(x, x') = \check{G}_{i\omega_n}(x, x') + \check{G}^{\mathrm{S}}_{i\omega_n}(x, x'), \tag{C6}$$

$$\check{G}^{\mathrm{S}}_{i\omega_n}(x, x') = \check{G}_{i\omega_n}(x, x_0)\,V\hat{\tau}_3\left[1 - \check{G}^{(0)}_{i\omega_n}(x_0, x_0)\,V\,\hat{\tau}_3\right]^{-1}\check{G}_{i\omega_n}(x_0, x'). \tag{C7}$$

The Green's function at the surface of a superconductor is calculated by taking the limit of $V \to \infty$. In the text, we input $x_0 = 0$ and analyze Eq. (C7) near the surface $0 < x \lesssim \xi_0$ and $0 < x' \lesssim \xi_0$, with $\xi_0 = \hbar v_F/\pi\Delta$ being the coherence length.

[1] Y. Tanaka and S. Kashiwaya, Phys. Rev. B **70**, 012507 (2004).
[2] Y. Asano, Y. Tanaka, and S. Kashiwaya, Phys. Rev. Lett. **96**, 097007 (2006).
[3] S. Ikegaya, Y. Asano, and Y. Tanaka, Phys. Rev. B **91**, 174511 (2015).
[4] S. Ikegaya and Y. Asano, J. Phys.: Condens. Matter **28**, 375702 (2016).
[5] S. Ikegaya, S.-I. Suzuki, Y. Tanaka, and Y. Asano, Phys. Rev. B **94**, 054512 (2016).
[6] M. Sato, Phys. Rev. B **73**, 214502 (2006).
[7] M. Sato and S. Fujimoto, Phys. Rev. B **79**, 094504 (2009).
[8] R. M. Lutchyn, J. D. Sau, and S. Das Sarma, Phys. Rev. Lett. **105**, 077001 (2010).
[9] Y. Oreg, G. Refael, and F. von Oppen, Phys. Rev. Lett. **105**, 177002 (2010).
[10] Y. Asano and Y. Tanaka, Phys. Rev. B **87**, 104513 (2013).
[11] S. Tamura and Y. Tanaka, Phys. Rev. B **99**, 184501 (2019).
[12] J. Linder and A. V. Balatsky, Rev. Mod. Phys. **91**, 045005 (2019).
[13] J. Cayao, C. Triola, and A. M. Black-Schaffer, Eur. Phys. J.: Spec. Top. **229**, 545 (2020).
[14] Y. Asano, Phys. Rev. B **64**, 014511 (2001).
[15] Y. Asano, J. Phys. Soc. Jpn. **71**, 905 (2002).
[16] Y. Tanaka, Y. V. Nazarov, and S. Kashiwaya, Phys. Rev. Lett. **90**, 167003 (2003).
[17] E. Bauer, G. Hilscher, H. Michor, C. Paul, E. W. Scheidt, A. Gribanov, Y. Seropegin, H. Noël, M. Sigrist, and P. Rogl, Phys. Rev. Lett. **92**, 027003 (2004).
[18] N. Reyren, S. Thiel, A. D. Caviglia, L. F. Kourkoutis, G. Hammerl, C. Richter, C. W. Schneider, T. Kopp, A.-S. Rüetschi, D. Jaccard, M. Gabay, D. A. Muller, J.-M. Triscone, and J. Mannhart, Science **317**, 1196 (2007).
[19] L. P. Gor'kov and E. I. Rashba, Phys. Rev. Lett. **87**, 037004 (2001).
[20] P. A. Frigeri, D. F. Agterberg, A. Koga, and M. Sigrist, Phys. Rev. Lett. **92**, 097001 (2004).
[21] S. Fujimoto, J. Phys. Soc. Jpn. **76**, 051008 (2007).
[22] C. R. Reeg and D. L. Maslov, Phys. Rev. B **92**, 134512 (2015).
[23] I. V. Bobkova and A. M. Bobkov, Phys. Rev. B **95**, 184518 (2017).
[24] J. Cayao and A. M. Black-Schaffer, Phys. Rev. B **98**, 075425 (2018).
[25] M. Sato, Y. Tanaka, K. Yada, and T. Yokoyama, Phys. Rev. B **83**, 224511 (2011).
[26] S. Ikegaya, S. Kobayashi, and Y. Asano, Phys. Rev. B **97**, 174501 (2018).
[27] J. Alicea, Phys. Rev. B **81**, 125318 (2010).
[28] J. You, C. H. Oh, and V. Vedral, Phys. Rev. B **87**, 054501 (2013).
[29] Y. Tanaka and A. A. Golubov, Phys. Rev. Lett. **98**, 037003 (2007).
[30] B. A. Bernevig, J. Orenstein, and S.-C. Zhang, Phys. Rev. Lett. **97**, 236601 (2006).
[31] J. Koralek, C. Weber, J. Orenstein, B. A. Bernevig, S.-C. Zhang, S. Mack, and D. D. Awschalom, Nature (London) **458**, 610 (2009).
[32] M. Kohda, V. Lechner, Y. Kunihashi, T. Dollinger, P. Olbrich, C. Schönhuber, I. Caspers, V. V. Bel'kov, L. E. Golub, D. Weiss, K. Richter, J. Nitta, and S. D. Ganichev, Phys. Rev. B **86**, 081306(R) (2012).
[33] M. P. Walser, C. Reichl, W. Wegscheider, and G. Salis, Nat. Phys. **8**, 757 (2012).
[34] J. Schliemann, Rev. Mod. Phys. **89**, 011001 (2017).